1.5-T MR imaging of pituitary microadenomas: technical considerations and CT correlation.

M V Kulkarni, K F Lee, C B McArdle, J W Yeakley and F L Haar

AJNR Am J Neuroradiol 1988, 9 (1) 5-11
http://www.ajnr.org/content/9/1/5

1.5-T MR Imaging of Pituitary Microadenomas: Technical Considerations and CT Correlation

Madan V. Kulkarni[1]
K. Francis Lee[1]
Craig B. McArdle[1]
Joel W. Yeakley[1]
Floyd L. Haar[2]

Thirty-seven patients with suspected pituitary tumors were evaluated prospectively with MR imaging at 1.5 T. MR detected a microadenoma at its correct location in all eight patients who underwent transsphenoidal surgery, while CT showed a focal abnormality in the correct location in only four of the eight patients. In patients who were clinically and endocrinologically considered to harbor a microadenoma, MR detected a focal pituitary signal abnormality in 83% and CT demonstrated a focal density abnormality in 42%. Infundibular displacement, focal gland convexity, and sellar-floor abnormality were seen equally well with CT and MR. MR imaging protocol included sagittal T1-weighted spin-echo, coronal inversion-recovery, and coronal spin-echo or cardiac-gated spin-echo images.

Although inversion-recovery images were superior in detecting focal pituitary lesions, some microadenomas were better seen on T2-weighted images. Cardiac-gated spin-echo images showed focal pituitary lesions better than ungated images did. Our technique demonstrates MR's superior sensitivity to CT in detecting a pituitary microadenoma.

CT has been widely used as an imaging method in the detection of pituitary tumors. High-resolution CT with IV contrast material, axial images with sagittal and coronal reformatting, and direct coronal imaging have shown the utility of CT in the imaging of the pituitary gland and its lesions [1–11]. Although indirect signs for the diagnosis of a pituitary microadenoma such as sellar floor erosion, focal convexity, and displacement of the infundibulum are well shown by CT, the detection of a focal hypo- or hyperdense lesion within the pituitary gland is the only statistically significant indicator of microadenoma [12]. However, microadenomas may reveal few or no abnormalities on CT [12, 13].

In recent years MR has also been useful in evaluating the pituitary gland [14–17]. High-resolution MR imaging has shown good results in the diagnosis of pituitary micro- and macroadenomas. However, in a recent comparative study, CT was found to be superior to MR in detecting microadenomas [18]. We prospectively evaluated patients with suspected pituitary tumors with MR and compared the results with available CT findings. The use of cardiac gated spin-echo and inversion-recovery techniques in diagnosing pituitary microadenomas was also evaluated. The imaging data were subsequently compared with clinical, endocrinological, and surgical data.

Subjects and Methods

Thirty-seven patients with suspected pituitary tumors were examined. Six patients had intrasellar lesions 10 mm or larger and were diagnosed as having pituitary macroadenomas. Of the 31 nonmacroadenoma patients (27 women, four men) 22 had increased prolactin and one had elevated adrenocorticotropic hormone. Amenorrhea, infertility, and/or galactorrhea were common symptoms in female patients. One male patient with impotence and three male patients with galactorrhea were found to have elevated prolactin levels (30–500 mg/ml). Two

Received May 27, 1987; accepted after revision August 12, 1987.

Presented at the annual meeting of the American Society of Neuroradiology, New York City, May 1987.

[1] Department of Radiology, University of Texas Medical School at Houston and Hermann Hospital, 6431 Fannin, 2.134 MSB, Houston, TX 77030. Address reprint requests to M. V. Kulkarni.

[2] Department of Neurosurgery, University of Texas Medical School at Houston and Hermann Hospital, Houston, TX 77030.

AJNR 9:5–11, January/February 1988
0195–6108/88/0901–0005

patients with headaches were initially evaluated by plain films and were suspected to have enlargement of sella turcica. These patients were then studied further with CT and MR. In both these patients and in six others with galactorrhea the pituitary hormone levels and thyrotropin-releasing hormone stimulation tests were normal.

All patients were evaluated with high-resolution MR studies performed on a 1.5-T GE Signa superconducting system. Imaging was performed in the sagittal and coronal planes with 3-mm slice thicknesses. There was a 0.6-mm gap between the slices. The field of view was 16 cm and the acquisition matrix was 256 × 128, which resulted in an in-plane resolution of 0.62 × 1.25 mm. The data were displayed on a 512^2 matrix. Sagittal T1-weighted images were acquired with the spin-echo technique with an echo time (TE) of 20 msec and repetition time (TR) of 800 msec. Coronal variable multiecho imaging was performed with TE = 20 and 80 msec and TR = 2000 msec. In 21 patients cardiac-gated spin-echo imaging was performed with an R-wave ECG trigger. Two sets of images were obtained, one with TE of 20 or 30 msec and the other with TE of 70 or 80 msec. The TR varied between 2000 to 3000 msec depending on the patient's heart rate. In seven patients coronal T2-weighted imaging was performed both with and without cardiac gating. In 11 patients additional cardiac-gated spin-echo or inversion-recovery imaging was performed in the sagittal plane. In 17 patients coronal T1-weighted images were obtained using a multislice inversion-recovery sequence with TE of 20 msec, inversion time (TI) of 800 msec, and TR of 2500. All acquisitions were performed with two excitations.

High-resolution CT scans were obtained in 14 patients from the nonmacroadenoma group with a GE 8800 or 9800 scanner. After obtaining a lateral scout image, rapid high-dose (80 g) meglumine diatrizoate* was administered IV. Axial contiguous slices through the pituitary gland were acquired with 1.5-mm collimation. This was followed by direct coronal images of the pituitary with 1.5-mm collimation. The axial images were reformatted in coronal and sagittal planes. In addition, eight CT scans in nonmacroadenoma patients were obtained at outside hospitals. After reevaluation, three of these scans were rejected because of either poor technique or absence of direct coronal pituitary images. Thus, a total of 19 high-resolution CT studies were available for comparison in the microadenoma group.

MR and CT scans were evaluated independently and blindly by two radiologists. All scans were evaluated for generalized or focal enlargement of the gland, focal convexity of diaphragma sellae, infundibular displacement, sellar floor erosion, sphenoid sinus septations, and presence or absence of focal lesions within the pituitary gland. Location of the abnormality was charted as anterior, middle, or posterior, as well as right, middle, or left, on the basis of available images in coronal and sagittal planes. Confidence levels for all findings were also recorded as 1 = normal, 2 = probably normal, 3 = maybe normal, 4 = probably abnormal, and 5 = definitely abnormal. In addition, T1-weighted, T2-weighted, and inversion-recovery images were assessed for their relative abilities in detecting focal lesions, as were gated and nongated spin-echo techniques.

Eight patients underwent transsphenoidal surgery of pituitary microadenomas. In these patients surgical and histologic findings were correlated with CT and MR. In the remaining 23 patients, the diagnosis, based on clinical presentation, endocrine evaluation, and response to therapy, was also correlated with CT and MR findings.

Results

Table 1 compares MR and CT in their ability to detect microadenomas in the surgical group. MR showed excellent sensitivity relative to CT in detecting focal lesions. Frequently the lesion was seen as an area of hypo- or isointensity surrounded by peripheral, increased signal intensity on T2-weighted images (Fig. 1). Either spin-echo or inversion-recovery T1-weighted images showed microadenomas as hypointense (Fig. 1B), except for one patient in whom a 6-mm microadenoma was seen as a hyperintense lesion both on T1- and T2-weighted images (Fig. 2). At surgery, a prolactinoma with central hemorrhage was found.

TABLE 1: MR and CT Findings in Surgically Proved Microadenomas

Finding	No. (n = 8) MR	CT
Focal lesions:		
True positive	8	4
False positive	0	1
Sellar floor ballooning	4	4
Focal convexity	4	3
Infundibular displacement	4	3

In the surgical group MR identified correctly the spatial location of microadenomas in all eight patients. CT showed a focal lesion in five of the eight patients. In one patient CT and MR identified a lesion, but CT identified the lesion on the left side while MR identified it on the right. During surgical exploration the lesion was identified only on the right. Thus, the CT scan in this patient was both false negative and false positive. In one patient with hyperprolactinemia and a normal CT scan on three previous occasions, MR detected a lesion in the left posterior part of the pituitary gland (Fig. 3). The infundibulum was deviated toward the side of the microadenoma. At surgical exploration, an excessive amount of bleeding was encountered and exposure was limited. The microadenoma was not seen by the surgeon. Therefore, the left posterior quadrant of the pituitary gland was removed because of MR findings. Histologic analysis confirmed the presence of a microadenoma at the MR-detected location. Of the four patients in whom CT failed to demonstrate a focal lesion correctly, indirect signs such as sellar floor erosion, deviation of infundibulum, and focal convexity were suggestive of a microadenoma in two. In four patients in whom CT and MR correctly identified microadenomas, MR made the diagnosis with a higher confidence level than CT in two of the four. Of eight patients with a surgically proved microadenoma, six had prolactinomas, one had a growth-hormone-secreting microadenoma, and one had a histologically proved luteinizing-hormone-secreting microadenoma.

In the nonsurgical group six patients who had intrasellar lesions 10 mm or larger were diagnosed as having pituitary macroadenomas. Of the remaining 23 patients, 15 were clinically believed to have hormone-producing pituitary lesions on the basis of clinical history, hormonal assay, and/or response to bromocriptine. Fourteen of these patients had hyperprolactinemia and one had increased adrenocorticotropic hormone. MR detected a focal lesion in 11 of these 15 patients. When the data were combined in the surgical and nonsurgical microadenoma groups, MR had a sensitivity of 82.6% while

* Berlex, Wayne, NJ.

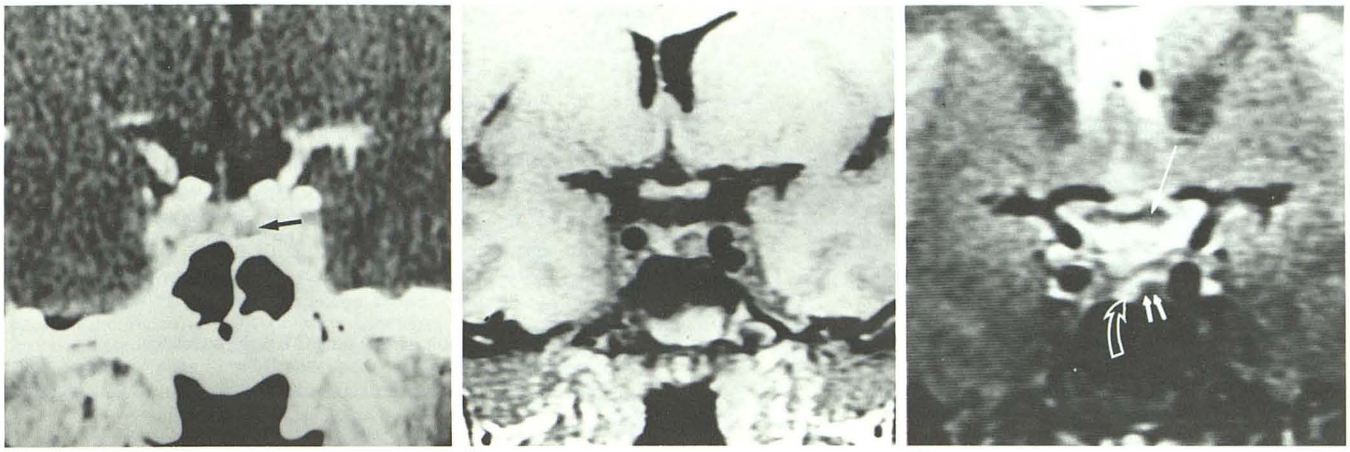

A B C

Fig. 1.—Coronal images in patient with surgically proved prolactin-secreting microadenoma.

A, CT scan at level of infundibulum shows suspicious hypodense lesion (*arrow*) in left side of pituitary gland near sellar floor. Lesion was reported as probably abnormal.

B, Inversion-recovery MR image at level of infundibulum shows definite focal lesion on left side. Peripheral part of lesion has decreased signal intensity relative to central part.

C, T2-weighted MR image with cardiac-gated spin-echo technique shows peripheral increased signal in prolactinoma (*open arrow*). Central hypointensity (*short solid arrows*) and chiasm (*long solid arrow*) are also seen. Also note excellent gray/white-matter differentiation in brain.

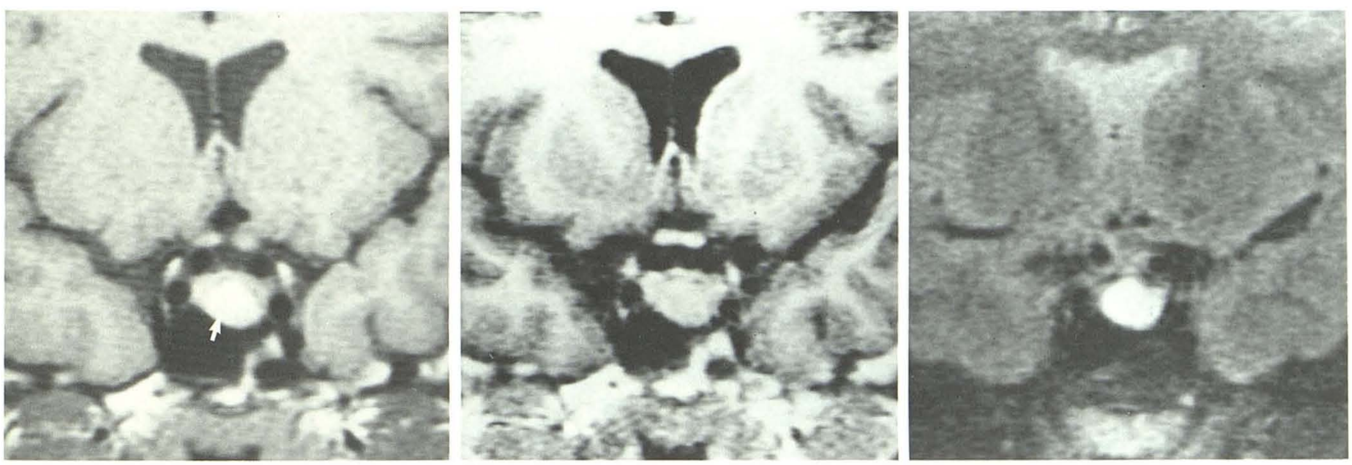

A B C

Fig. 2.—Coronal MR images in 22-year-old man with surgically proved prolactinoma with central hemorrhage.

A, T1-weighted spin-echo MR image (TR = 800 msec, TE = 20 msec) shows sellar-floor ballooning toward left. Increased signal intensity centrally (*arrow*) represents subacute hemorrhage.

B, Inversion recovery MR image shows similar contour of intrasellar tissue, but area of hemorrhage is isointense relative to residual pituitary gland.

C, Nongated T2-weighted MR image shows markedly increased signal from hemorrhagic prolactinoma. Gray/white-matter contrast is poor.

CT had a sensitivity of 42.1% in demonstrating a focal lesion. Table 2 demonstrates the relative incidences of focal lesions, sellar floor erosion, infundibular displacement, and focal convexities seen on CT and MR. After extensive clinical and hormonal evaluation eight patients were considered endocrinologically normal, although MR detected a microadenoma in three of these patients (Fig. 4).

Of 23 patients in whom a microadenoma was detected by MR, in 17 imaging was performed with three pulse sequences: T1-weighted spin echo, T1-weighted inversion recovery, and T2-weighted cardiac-gated spin echo. In 10 of the 17, the focal abnormality was best seen on inversion recovery, in six on cardiac-gated spin echo, and in one on T1-weighted spin echo. In seven patients who had both cardiac-gated and nongated spin-echo images, five of seven had a focal lesion detected on cardiac-gated spin-echo and three of seven had a focal lesion diagnosed on nongated T2-weighted spin-echo images. In three patients with focal lesions on both cardiac-

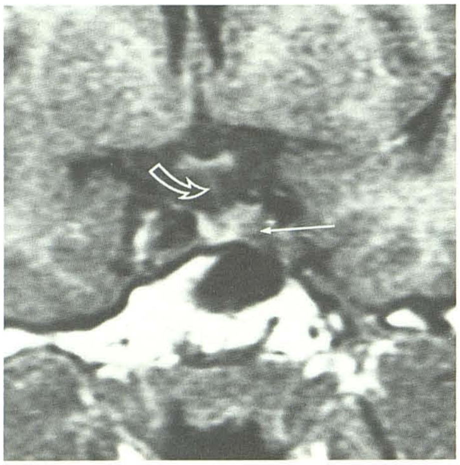

Fig. 3.—Inversion-recovery MR image in coronal plane shows focal hypointensity (*solid arrow*) in prolactinoma. Infundibulum (*open arrow*) is deviated toward adenoma. CT scans on three previous occasions and T2-weighted MR image did not reveal focal lesions.

gated and nongated spin-echo images, the diagnosis of focal abnormality was made with a higher confidence level on cardiac-gated images (Fig. 5). In 15 of 17 microadenomas detected on T2-weighted images, the lesion was seen because of the presence of a peripheral rim of increased signal intensity. This rim was seen better on cardiac-gated images (Fig. 5). In 11 patients additional imaging was performed in the sagittal plane with cardiac-gated spin-echo or inversion-recovery sequences. In only three of seven patients with a microadenoma in this group were the sagittal images believed

TABLE 2: Sensitivities of MR and CT in Assessing Microadenomas

Finding	% Sensitivity	
	MR (n = 23)	CT (n = 19)
Focal lesion	82.6	42.1
Sellar floor abnormality	43.4	47.3
Focal convexity	43.4	36.8
Infundibular displacement	39.1	31.6

Note.—Sensitivities were assessed on the basis of surgical and endocrinological data.

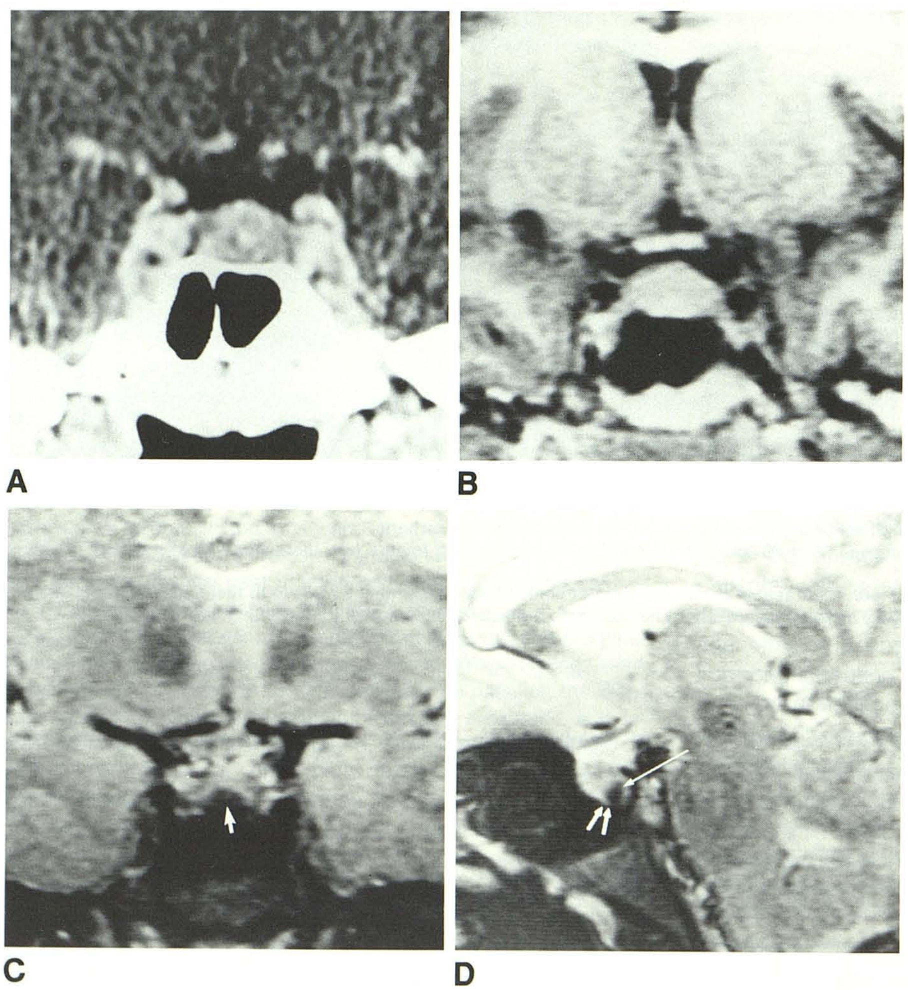

Fig. 4.—24-year-old woman with galactorrhea. After extensive endocrinologic evaluation, no hormonal abnormality was detected.

A, Coronal CT scan shows focal central convexity of pituitary superiorly but no focal density abnormality.

B, Coronal inversion-recovery MR image also shows focal convexity but no evidence of focal signal abnormality.

C, T2-weighted cardiac-gated spin-echo MR image shows focal hypointensity (*arrow*) surrounded by hyperintense signal.

D, Sagittal plane better shows focal hypointense lesion (*long arrow*) and mild sellar floor ballooning (*short arrows*). (Sagittal inversion-recovery MR image at same level did not show focal signal abnormality.)

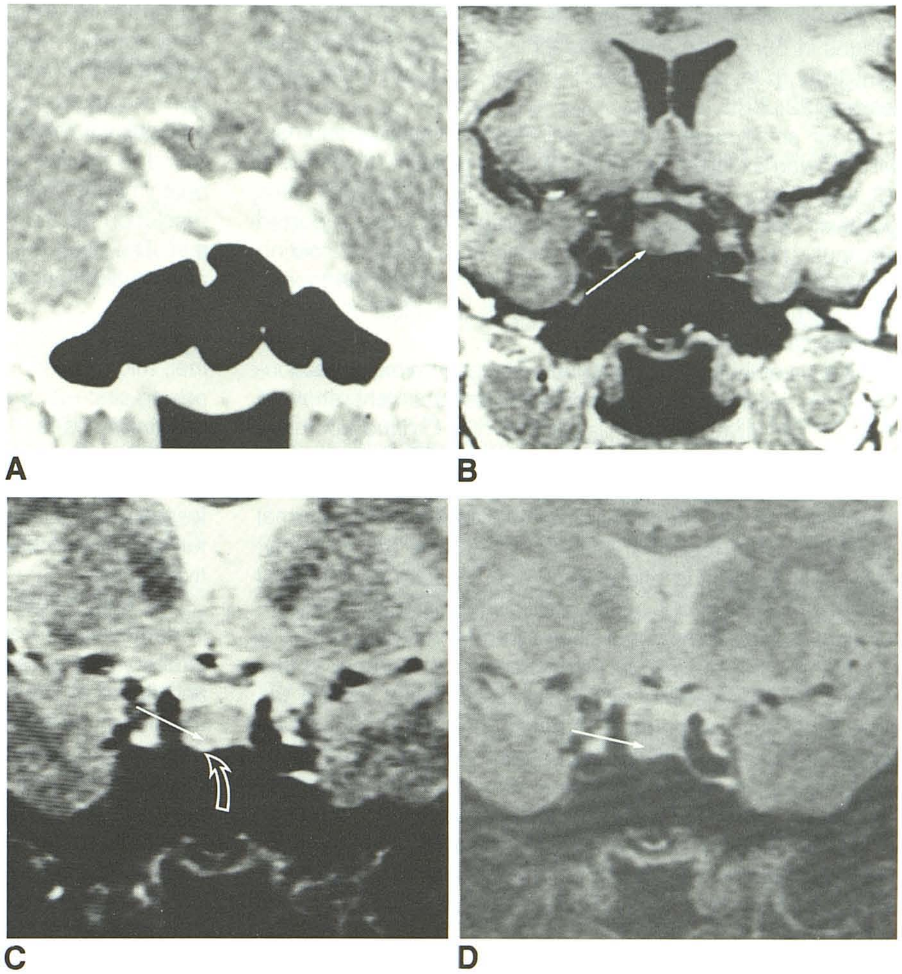

Fig. 5.—Coronal images in 37-year-old woman with galactorrhea, amenorrhea, and hyperprolactinemia.

A, CT scan was reported to be normal. Linear streak artifact was noted in right side of gland.

B, T1-weighted inversion-recovery MR image shows convexity superiorly. Focal lesion is noted near sellar floor (*arrow*). Peripheral portion of lesion is hypointense.

C, T2-weighted cardiac-gated spin-echo MR image shows central focal hypointensity (*solid arrow*) surrounded by peripheral hyperintensity. Sellar floor ballooning is seen on right (*open arrow*).

D, Nongated T2-weighted MR image shows faintly focal lesion (*arrow*). Contrast between lesion and normal pituitary gland as well as gray/white-matter is poor. Lesion was seen retrospectively on CT.

to have provided additional diagnostic information not available on the coronal images.

Discussion

CT with high-resolution techniques has recently been the imaging method of choice in the diagnosis of pituitary abnormalities [1–4, 7–11]. Diagnosis is usually made by the presence of a hypo- or hyperdense lesion within the pituitary gland after IV contrast enhancement. Indirect signs of a microadenoma, such as infundibular displacement, focal convexity, and sellar floor abnormality, are also sometimes helpful in making the diagnosis, but a focal hypo- or hyperdense lesion is reported to be the only statistically significant indicator for microadenomas [12]. In one series 43% of surgically proved microadenomas were found to be isodense on high-resolution contrast-enhanced CT [12]. On the other hand, the presence of inhomogeneities within the pituitary gland and artifacts frequently makes the CT evaluation of small microadenomas difficult [12, 19, 20].

Recently, MR imaging has been used in the diagnosis of sellar and juxtasellar pathology [14–18]. Various imaging techniques have been described for imaging pituitary lesions. In a recent study, MR was found to be superior to CT in the diagnosis of pituitary macroadenomas, but MR was reported to be less sensitive than CT in identifying discrete microadenomas within the pituitary gland [18]. The difference in MR sensitivities in the detection of microadenomas between that report and our current study probably reflects the MR technique. Technical considerations in MR are as important as those involved with high-resolution CT [12].

Pituitary macroadenomas and large sellar and juxtasellar lesions can be seen to better advantage with MR because of excellent inherent contrast relative to surrounding structures. Detection of microadenomas in normal-sized or minimally enlarged pituitary glands probably requires high-resolution techniques. We used spin-echo and inversion-recovery sequences with the smallest slice thicknesses available with our system (3 mm) and decreased the field of view to 14–16 cm, resulting in a small voxel volume to improve spatial resolution [21]. In addition, cardiac-gated spin-echo images improve contrast between the microadenoma and surrounding pituitary gland by diminishing ghosting artifacts seen along the phase-encoding axis. This improvement is demonstrated by superior definition of the gray/white-matter junction on cardiac-gated images compared with nongated spin-echo images in our series. Similar techniques have shown better sensitivity in lesion detection in spinal cord and intracranial lesions [22, 23].

In our small series of surgically proved microadenomas, MR showed excellent sensitivity with no false-positive cases. CT identified lesions correctly in 50%; there was one false positive. Our CT results are comparable to those reported previously [12, 13]. The superior sensitivity of MR in detecting focal pituitary lesions is also reflected in the group diagnosed as having microadenomas on the basis of clinical and endocrinological evaluation.

Analysis of indirect signs, such as focal convexity, ballooning of the sellar floor, and infundibular displacement, showed that MR sensitivity was similar to that of CT. Although these signs are sometimes helpful, the diagnosis of microadenoma on the basis of these indirect signs is imprecise. Slight displacement of the infundibulum with a histologically normal gland has been reported in anatomic studies [6]. Similarly, sellar-floor ballooning and erosion can be seen as a normal variant [24–27]. In our series, sellar-floor ballooning and infundibular displacement were seen with MR in 43% and 39% of patients, respectively, in the microadenoma group. In one patient (Fig. 3), the infundibulum was displaced toward the side of the microadenoma. This patient had been treated with bromocriptine for 3 years. The infundibular displacement is presumed to be from hemorrhage and subsequent scarring secondary to bromocriptine therapy [28], leading to retraction of the infundibulum toward the side of the microadenoma. At the time of the MR study no hemorrhage was seen. Similarly, focal convexity of the gland was seen on MR in 10 of 23 patients with microadenoma.

The selection of proper technique and pulse sequence is also valuable. In our series the inversion-recovery sequence was superior in detecting focal lesions, but in some patients the lesions were not seen on inversion-recovery and were detected on T2-weighted images. On T2-weighted images the lesion was detected on the basis of peripheral, increased signal intensity, while focal microadenomas were frequently mildly hypo- or isointense relative to the pituitary. Cardiac-gated spin-echo images reduced the phase-encoding artifacts generated by intracavernous carotid and CSF pulsatile motion, resulting in superior demonstration of the peripheral increased signal. It is also important to note that focal convexity and infundibular displacement were better appreciated on inversion-recovery or T1-weighted images when compared with cardiac-gated spin-echo images. Short TE, long TR images offered superior visualization of sphenoid sinus septations. Although the CT demonstration of the presence of bony septa in the sphenoid sinus was excellent, MR images with short TEs and long TRs also showed them adequately for planning transsphenoidal surgery.

As described by Kucharczyk et al. [17], changing the window width to a narrow display window will sometimes help discriminate the hypointensity within the adenoma from surrounding pituitary gland. Similarly, changes in display window width and level enhance visualization of septations within the sphenoid sinus.

Coronal inversion recovery and T2-weighting with sagittal T1-weighting were adequate in 24 of 31 patients. In 11 patients additional inversion-recovery or T2-weighted images were acquired in the sagittal plane. Only in three of seven patients with microadenomas were the sagittal images believed to provide additional information not available on coronal images. The data acquisition time for routine high-resolution pituitary MR at our institution is approximately 26 min. The need for additional sagittal imaging can be decided after evaluation of coronal images; they are not necessary routinely.

In three of eight patients who were endocrinologically normal, microadenomas were detected on MR. This is not surprising since 22.5–45% of endocrinologically normal patients in autopsy series were found to have a microadenoma [29–31]. This may be a "null-cell" adenoma or prolactinoma, which is endocrinologically inactive. MR could be an imaging method for the diagnosis and follow-up in these patients to determine tumor size and biological behavior in endocrinologically inactive tumors.

Our early experience suggests that MR is superior to CT in detecting a focal lesion in patients suspected of having a pituitary microadenoma. The differences between our results and those of Davis et al. [18] probably can be attributed to the difference in technique, especially slice thickness, and the use of cardiac-gated spin-echo and inversion-recovery sequences. MR not only allows the use of multiple imaging planes directly, but also a variety of pulse sequences can be used until satisfactory diagnosis is achieved. With bolus contrast-enhanced CT, on the other hand, only one attempt to obtain a satisfactory study is possible during one patient visit. The routine MR pituitary microadenoma protocol (Table 1) requires 26–30 min of data acquisition and is tolerated extremely well. Thus, MR will probably replace CT as a screening method for suspected pituitary microadenomas.

ACKNOWLEDGMENTS

We thank Cynthia Brewer, Michael Blackburn, and Elizabeth Berry for technical assistance and Toni A. Jones for manuscript preparation.

REFERENCES

1. Syvertsen A, Haughton VM, Williams AL, Cusick JF. The computed tomographic appearance of the normal gland and pituitary microadenomas. *Radiology* **1979**;133:385–391
2. Wolpert SM, Post KD, Biller BJ, Molitch ME. The value of computed tomography in evaluating patients with prolactinoma. *Radiology* **1979**;131:117–119
3. Newton DR, Witz S, Norman D, Newton TH. Economic impact of CT scanning on the evaluation of pituitary adenomas. *AJNR* **1983**;4:57–60, *AJR* **1983**;140:573–576
4. Kricheff II. The radiologic diagnosis of pituitary adenoma. *Radiology* **1979**;131:263–265
5. Roppolo HM, Latchaw RE, Meyer JD, Curtin HD. Normal pituitary gland: 1. Macroscopic anatomy-CT correlation. *AJNR* **1983**;4:927–935
6. Ropollo HM, Latchaw RE. Normal pituitary gland: 2. Microscopic anatomy-CT correlation. *AJNR* **1983**;4:937–944
7. Woodruff WW, Heinz ER, Djang WT, Voorhees D. Hyperprolactinemia: an

unusual manifestation of suprasellar cystic lesions. *AJNR* **1987**;8:113–116
8. Daniels DL, Williams AL, Thorton RS, Meyer GA, Cusick JF, Haughton VM. Differential diagnosis of intrasellar tumors by computed tomography. *Radiology* **1981**;141:697–701
9. Hemminghytt S, Kalkhoff RK, Daniels DL, Williams AL, Grogan JP, Haughton VM. Computed tomographic study of hormone secreting microadenomas. *Radiology* **1983**;146:65–69
10. Swartz JD, Russell KB, Basile BA, O'Donnell PC, Poply GL. High resolution computed tomographic appearance of the intrasellar content in women of childbearing age. *Radiology* **1983**;147:115–117
11. Bonneville JF, Cattin F, Moussa-Bacha K, Portha C. Dynamic computed tomography of the pituitary gland: the tuft sign. *Radiology* **1983**;149:145–148
12. Davis PC, Hoffman JC Jr, Tindall GT, Braun IF. Prolactin-secreting pituitary microadenomas: inaccuracy of high-resolution CT imaging. *AJNR* **1984**;5:721–726, *AJR* **1985**;144:151–156.
13. Davis PC, Hoffman JC Jr, Tindall GT, Braun IF. CT-surgical correlation of pituitary adenomas: evaluation of 133 patients. *AJNR* **1985**;6:711–716
14. Hawkes RC, Holland GN, Moore WS, Corston R, Kean DM, Worthington BS. The application of NMR imaging to the evaluation of pituitary and juxtrasellar tumors. *AJNR* **1983**;4:221–222
15. Bilaniuk LT, Zimmerman RA, Wehrli FW, et al. Magnetic resonance imaging of pituitary lesions using 1.0 to 1.5 T field strength. *Radiology* **1984**;153:415–418
16. Oot R, New PF, Buonanno FS, et al. MR imaging of pituitary adenomas using a prototype resistive magnet: preliminary assessment. *AJNR* **1984**;5:131–137
17. Kucharczyk W, Davis DO, Kelly WM, Sze G, Norman D, Newton TH. Pituitary adenomas: high resolution MR imaging at 1.5 T. *Radiology* **1986**;161:761–765
18. Davis PC, Hoffman JC, Jr, Spencer T, Tindall GT, Braun IF. MR imaging of pituitary adenoma: CT, clinical and surgical correlation. *AJNR* **1987**;8:107–112
19. Chambers EF, Turski PA, LaMaster D, Newton TH. Regions of low density in the contrast enhanced pituitary gland: normal and pathologic processes. *Radiology* **1982**;144:109–113
20. Earnest F, McCullough EC, Frank DA. Fact of artifact: an analysis of artifact in high resolution computed tomographic scanning of the sella. *Radiology* **1981**;140:109–113
21. Kulkarni MV, Patton JA, Price RR. Technical considerations for the use of surface coils in MRI. *AJR* **1986**;147:373–378
22. Enzmann DR, Rubin JB, Wright A. Use of cerebrospinal fluid gating to improve T2-weighted images. Part I. The spinal cord. *Radiology* **1987**;162:763–767
23. Enzmann DR, Rubin JB, O'Donohue J, Griffin C. Drace J, Wright A. Use of cerebrospinal fluid gating to improve T2-weighted images. Part II. Temporal lobes, basal ganglia and brain stem. *Radiology* **1987**;162:768–773
24. Bruneton JN, Drouillard JP, Sabatier JC, Elie GP, Tavernier JF. Normal variants of the sella turcica. *Radiology* **1979**;131:99–104
25. Dubois PJ, Orr DP, Hoy RJ, Herbert DL, Heinz ER. Normal sellar variations in frontal tomograms. *Radiology* **1979**;131:105–110
26. Burrow GN, Wortzman G, Rewcastle NB, Holgate RC, Kovaks K. Microadenomas of the pituitary and abnormal sellar tomograms in an unselected autopsy series. *N Engl J Med* **1981**;304:156–158
27. Raji MR, Kishore PR, Becker DP. Pituitary microadenoma: a radiological-surgical correlative study. *Radiology* **1981**;139:95–99.
28. Weissbuch SS. Explanation and implications of MR signal changes within pituitary adenomas after Bromocriptine therapy. *AJNR* **1986**;7:214–216
29. McComb DJ, Ryan N, Horvath E, Kovacs K. Subclinical adenomas of the human pituitary. *Arch Pathol Lab Med* **1983**;107:488–491
30. Parent D, Brown B, Smith EE. Incidental pituitary adenomas: a retrospective study. *Surgery* **1982**;92:880–883
31. Taylor CR, Jaffe CC. Methodological problems in clinical radiology research: pituitary microadenoma detection as a paradigm. *Radiology* **1983**;147:279–283